Synthesis and Structural Insight into Poly(dimethylsiloxane)-b-Poly(2-vinylpyridine) Copolymers

Gkreti-Maria Manesi, Ioannis Moutsios, Dimitrios Moschovas, Georgios Papadopoulos, Christos Ntaras, Martin Rosenthal, Loic Vidal, Georgiy G Ageev, Dimitri A Ivanov, Apostolos Avgeropoulos

polymers

MDPI

Article

Synthesis and Structural Insight into Poly(dimethylsiloxane)-*b*-Poly(2-vinylpyridine) Copolymers

Gkreti-Maria Manesi[1], Ioannis Moutsios[1,2], Dimitrios Moschovas[1], Georgios Papadopoulos[1], Christos Ntaras[1], Martin Rosenthal[3], Loic Vidal[2], Georgiy G. Ageev[4], Dimitri A. Ivanov[2,4,5,6] and Apostolos Avgeropoulos*[1,5]

[1] Department of Materials Science & Engineering, University of Ioannina, University Campus-Dourouti, 45110 Ioannina, Greece; gretimanesi@uoi.gr (G.-M.M.); imoutsios@uoi.gr (I.M.); dmoschov@uoi.gr (D.M.); gpap414@gmail.com (G.P.); (C.N.)
[2] Institut de Sciences des Matériaux de Mulhouse – IS2M, CNRS UMR7361, 15 Jean Starcky, Mulhouse 68057, France; loic.vidal@uha.fr (L.V.); dimitri.ivanov@uha.fr (D.A.I.)
[3] Department of Chemistry, KU Leuven, Celestijnenlaan 200F, Box 2404, B-3001 Leuven, Belgium; martin.rosenthal@esrf.fr (M.R.)
[4] Sirius University of Science and Technology, 1 Olympic Ave, 354340, Sochi, Russia;
[5] Faculty of Chemistry, Lomonosov Moscow State University (MSU), GSP-1, 1-3 Leninskiye Gory, 119991 Moscow, Russia;
[6] Federal Research Center of Problems of Chemical Physics and Medicinal Chemistry RAS, Russian Academy of Sciences, Chernogolovka, 142432 Moscow, Russia;

* Correspondence: aavger@uoi.gr (A.A.);

Abstract: In this study the exploitation of anionic polymerization for the synthesis of living poly(dimethylsiloxane) or PDMS as well as poly(2-vinylpyridine) or P2VP homopolymers and the subsequent use of chlorosilane chemistry in order to be covalently joined leading to PDMS-*b*-P2VP copolymers is proposed. The thorough manipulations under high vacuum conditions using highly rinsed apparatuses and reagents enabled the synthesis of well-defined materials in terms of molecular as well as compositional homogeneity. The number average molecular weights, dispersity indices and thermal transitions were determined through size exclusion chromatography (SEC), proton nuclear magnetic resonance spectroscopy (^{1}H NMR) and differential scanning calorimetry (DSC), respectively. The morphological characterization results suggested that for common composition ratios lamellar, cylindrical and spherical phases with domain periodicities ranging from approximately 15 to 39 nm are formed. A post polymerization chemical modification reaction to quaternize some of the pyridine rings in the copolymer with the highest P2VP content is also reported. Additional characterizations on the modified copolymer including ^{1}H NMR, infrared spectroscopy, DSC and contact angle were conducted. The synthesis, characterization and introduction of positive charged groups into the copolymer structure are important findings towards the preparation of functional materials for various applications.

Keywords: high χ copolymers; anionic polymerization; chlorosilane chemistry; PDMS; P2VP; divergent T_gs; self-assembly behavior; quaternization

Citation: To be added by editorial staff during production.

Academic Editor: Firstname Lastname

Received: date
Revised: date
Accepted: date
Published: date

1. Introduction

To obtain well-defined and stable nanostructures with extremely low dimensions for nanotechnology purposes highly immiscible copolymers should be designed [1,2]. Inherent properties including thermal stability, etching selectivity, post-polymerization chemical modification capability and high-throughput synthesis are of great significance [1-4].

Silicon-containing copolymers have a leading role in various applications because they showcase the aforementioned characteristics [2]. This fact has motivated the scien-

tific community towards the synthesis of versatile copolymer combinations which include at least one inorganic segment. Several poly(dimethylsiloxane) or PDMS-based copolymers such as PS-*b*-PDMS [5,6], PDMS-*b*-P2VP [7], PDMS-*b*-P4VP [8], PDMS-*b*-PLA [9], PDMS-*b*-PMMA [10], P3HS-*b*-PDMS [11] and PDMS-*b*-PEO [12] [where PS: polystyrene, P2VP: poly(2-vinylpyridine), P4VP: poly(4-vinylpyridine), PLA: poly(lactid acid), PMMA: poly(methyl methacrylate), P3HS: poly(3-hydroxystyrene) and PEO: poly(ethylene oxide] have been synthesized using living anionic, control radical polymerization techniques, ring opening polymerization or azide-alkyne "click" reactions.

Poly(vinylpyridine)-based copolymers are highly versatile materials due to the chemical modification capability of the pyridinyl nitrogen atoms in the –ortho or –para positions [13-15]. Significant studies have shed light on the properties afforded after the reactions which induce an electron-rich backbone and electron-poor pyridiniums for different quaternization degrees. It is straightforward that the properties and therefore the targeted application are dependent on the percentage of quaternization [13-15].

Notwithstanding the fact that the advent of new synthetic approaches has enabled the fabrication of different systems, the synthesis of PDMS-*b*-P2VP remains largely unexplored. Lee et al. [16] proposed certain synthetic protocols for the synthesis of linear diblock and triblock copolymers of the AB and ABA types (where A: P2VP and B: PDMS) that involved the use of an organolithium compound as initiator or a reagent with combined alkylating and acetal functional groups. Fragouli et al [17] reported the synthesis of tetrablock quarterpolymers of the PS-*b*-PI-*b*-PDMS-*b*-P2VP [PI: poly(isoprene)] through anionic polymerization followed by coupling with a selective heterofunctional linking chlorosilane agent (chloromethylphenylethylenedimethylchlorosilane). Reversible addition fragmentation chain transfer (RAFT) polymerization was employed quite recently by Hur et al. [18] for the synthesis of low molecular weight copolymers of the specific type. Only limited research works report the synthesis of the specific sequence but its great potential is displayed in a work by Jeong et al. [7] in which the self-assembly behavior in thin films after exposure to different solvents, in a process widely established as solvent vapor annealing, was studied. Also, the self-assembly behavior of a PDMS-*b*-P2VP copolymer in thin films using pre-patterned substrates coated with different brushes was studied to evaluate the minimum value of line edge and/or width roughness [19]. A different research involved the fabrication of silicon oxide dots and the incorporation of gold nanoparticles in the polymeric matrix [20]. The bulk phase behavior prior and after blending with 1-pyrenebutyric acid towards the formation of complexes through non-covalent interactions between the nitrogen of P2VP monomeric units and the butyric acid functional group as the temperature varied was examined by Shi et al [21].

In our work an alternative synthetic approach for the preparation of linear PDMS-*b*-P2VP copolymers is proposed. Living anionic polymerization was utilized for the synthesis of both PDMS and P2VP homopolymers which were then coupled using an appropriate reagent through chlorosilane chemistry. To combine the specific segments is rather challenging due to the quite different synthetic protocols followed during the polymerization. Restrictions related to electron affinity and weak nucleophilicity in conjunction with the strict purification protocols should be taken under consideration. The molecular characteristics of the involved segments including the dispersity indices and total number average molecular weights as well as the successful synthesis were determined using size exclusion chromatography (SEC). The mass as well as the volume fraction ratios were calculated using ^{1}H NMR (proton nuclear magnetic resonance spectroscopy) experiments, while the thermal behavior was studied using differential scanning calorimetry (DSC). Two distinct glass transition temperatures corresponding to the PDMS and P2VP blocks were recorded indicating the strong repelling forces between them. Lamellar, cylindrical and spherical phases with dimensions ranging from approximately 15 to 39 nm were formed in bulk as indicated by the morphological characterization through transmission electron microscopy (TEM) and small angle X-ray scat-

tering (SAXS). Also, a post polymerization chemical modification reaction towards the formation of a quaternized copolymer derivative was carried out to the sample with the highest P2VP content. The molecular, thermal and wetting properties after the quaternization were determined to map any alternation induced due to the existence of positive charge in some monomeric units of the P2VP segment.

2. Materials and Methods

2.1 Materials

The solvents (benzene, tetrahydrofuran, methanol, chloroform and n-hexanes), monomers [1,1-diphenylethylene, 2-vinyl pyridine (2-VP) and hexamethylcyclotrisiloxane (D_3)], coupling agent [dichlorodimethylsilane], initiators [*normal*-BuLi (*n*-BuLi), *secondary*-BuLi (*sec*-BuLi)] and drying agents (calcium hydride and triethylaluminum) have been provided by Sigma-Aldrich (Sigma-Aldrich Co., St. Louis, MO, USA) as well as the alkyl halide used in the quaternization (bromoethane) reaction. The purification procedures of all solvents and coupling agent were performed according to the demanding protocols of anionic polymerization, already described in the relative literature [22]. The apparatuses were meticulously rinsed with *n*-BuLi to eliminate any contaminants prior to any reaction. 2-VP was purified twice by calcium hydride prior to distillation to sodium mirror and finally to triethylaluminum [22,23]. D_3 was dissolved in benzene, then was purified over calcium hydride as well as over living polystyrene lithium [$PS^{(-)}Li^{(+)}$ at least twice] chains and stored to pre-calibrated ampoules [5,22].

2.2 Synthesis Protocols

The procedure is realized by polymerizing the hexamethylcyclotrisiloxane (6.0 g, 0.08 mol) with *sec*-BuLi (1.13 mmol) in the presence of non-polar solvent (benzene ~200 ml) followed by the addition of a polar solvent (tetrahydrofuran ~200 ml) in a 1:1 ratio after seven days at cryogenic conditions (−20 °C) as thoroughly elaborated in the literature [5,6]. Through this protocol the conversion of monomer approaches 100% with minimum side reactions, which is critical for the effective coupling of the living PDMS homopolymer with the dimethyldichlorosilane.

The molar ratio of coupling agent towards the $PDMS^{-}Li^{+}$ is in significant excess (at least 500-fold, 0.57 mol) to ensure the substitution of only one chlorine atom [22, 24,25]. The excess of coupling agent was removed under high vacuum and the intermediate PDMS-$Si(CH_3)_2Cl$ product was washed with purified benzene, dissolved in tetrahydrofuran and kept at low temperature. The P2VP homopolymer was prepared in a different apparatus which was meticulously rinsed with a bis phenyl hexyl lithium solution. 2-vinyl pyridine (6.0 g, 0.06 mol) and *sec*-BuLi reacted in presence of tetrahydrofuran at −78 °C for 1 hour using a nitrogen/isopropyl alcohol bath. The final step involved the coupling of the intermediate PDMS-$Si(CH_3)_2Cl$ product and the living P2VP block. To control the instability of the materials at increased temperatures the new apparatus with the attached vessels containing the two different segments is placed for approximately 15 minutes at −20 °C and subsequently the break-seal is ruptured towards the coupling of the macromolecular chains. The solution was left under stirring for approximately two weeks where the gradual discoloration of the solution was apparent prior to the precipitation to cold stabilized methanol. The details concerning the purification protocols and synthesis protocols are ascribed to the DVP-1 (see Table 1). Manipulating the monomers and/or initiator quantities but keeping coherent synthetic protocols the remaining samples were synthesized. Note that after the completion of each synthetic step aliquots were retrieved to determine the molecular characteristics and justify the successful reactions. Figure 1 summarizes all the reactions that took place for clarification reasons.

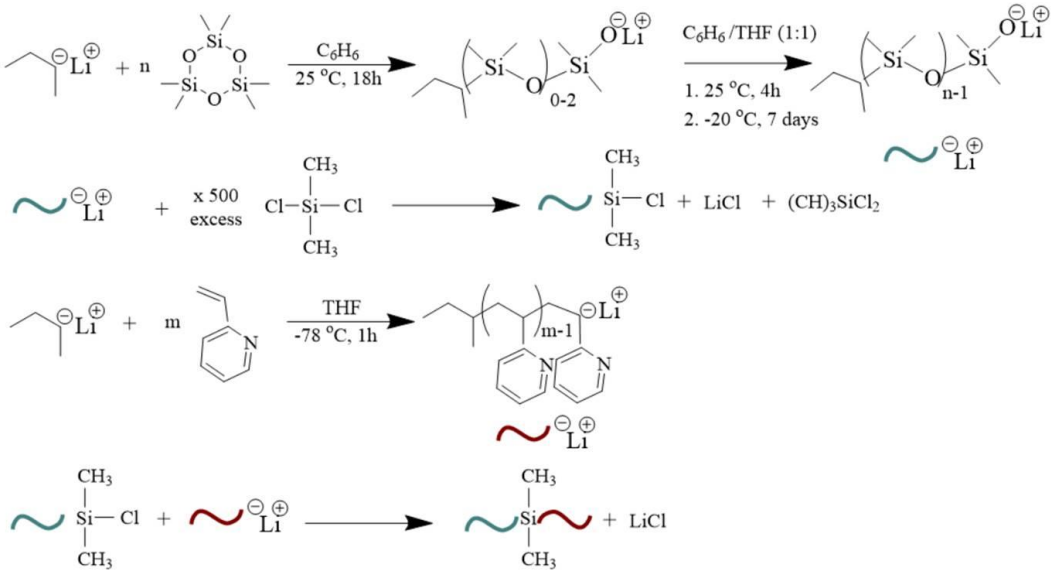

Figure 1. Synthesis reactions for the preparation of PDMS-*b*-P2VP copolymers involving different steps, meaning the polymerization of D_3 towards the formation of living PDMS chains, the coupling of $PDMSLi^+$ with dichlorodimethylsilane, the polymerization of 2-VP towards the formation of living P2VP chains and finally the coupling of the chlorosilane terminated PDMS homopolymer with the active P2VP chains.

Concerning the post-polymerization chemical modification reaction towards the formation of PDMS-*b*-[P2VP-*r*-poly(1-ethyl-2-vinylpyridinium bromide)] 1.0 g of DVP-3 (see Table 1) was vigorously stirred with excess (with respect to the concentration of the pyridine units) of bromoethane (3.2 mL) under reflux for 16 hours prior to purification based on a previous study conducted by our research group [15].

2.3 Methods

A fully Integrated GPC System (PL-GPC 50) from Agilent Technologies (Agilent Technologies/Polymer Labs, St. Clara, CA, USA), with an isocratic pump (1.0 ml/min), a three-column [three columns in series (PLgel 5 mm Mixed-C, 300 x 7.5 mm) capacity oven (LabAlliance) operating at 35 °C, refractive index (RI, Shodex RI-101) and ultraviolet absorbance (UV, SpectraSystem UV1000) detectors was used. The eluent was stabilized (2% v/v triethylamine) THF and the calibration took place using eight PS standards (M_P: 4,830 to 3,242,000 g/mol)].

^{1}H NMR spectra were recorded in deuterated chloroform at 25 °C using Bruker AVANCE II spectrometers (Bruker GmbH, Berlin, Germany) operating at 250 MHz. An UXNMR (Bruker) software was used in the data analysis. The quaternized sample was recorded in deuterated dimethyl sulfoxide (DMSO-d_6) at 25°C.

DSC measurements were carried out on a *Q*20 TA instrument (TA Instruments Ltd., Leatherhead, UK) from −140 °C to 140 °C at a 10 °C/min heating rate. From the three cycles (two heating and one cooling) conducted, the presented thermographs correspond to the second heating and were processed using Advantage v5.4.0 (TA instruments) software.

A Nicolet Nexus 670 (Wake Forest, NC, USA) infrared spectrometer equipped with a single horizontal golden gate attenuated total reflectance (ATR) cell was used for the FT-IR measurements. Spectra were recorded by averaging 64 scans between 4000 and 400 cm^{-1} with a resolution of 2 cm^{-1} under ambient conditions.

A contact angle instrument (OCA 25, DataPhysics Instruments GmbH, Filderstadt, Germany) was used to study the wetting properties. Samples were initially dissolved in chloroform (3 wt% solution) and were spin casted onto silicon wafers [treated with piranha solution (sulfuric acid/hydrogen peroxide: 3/1)] at ambient conditions using 3700

rpm for 30 s to obtain films with ~50 nm thickness. Five separate measurements in five different regions were conducted and the average value was calculated and presented. The deviation was ±2°.

A JEOL JEM 2100-HR, 200 KeV electron microscope (JEOL Ltd., Tokyo, Japan) was utilized for the TEM studies. Prior to TEM experiments, samples were cast from a dilute 5 wt% solution in chloroform and the solvent evaporation was completed after 7 days. The obtained ultra-thin sections (ca. 50 nm thick) from a Leica EM UC7 ultramicrotome (Leica EM UC7 from Leica Microsystems, Wetzlar, Germany) at −140 °C, were placed on 600 mesh copper grids.

Small angle x-ray scattering (SAXS) experiments were performed on a Xenocs Xeuss SAXS/WAXS system equipped with a GeniX3D copper microfocus tube operating at 60 kV and 0.59 mA. All samples were placed in an evacuated chamber and illuminated with monochromatic X-rays in transmission geometry. The scattered intensity was recorded using a Dectris Pilatus 300k detector located 2.2 m downstream the sample position. Small-angle X-ray scattering experiments were also conducted at the BM26 beamline of the ESRF (Grenoble).

3. Results and Discussion

Through anionic polymerization and chlorosilane chemistry, segments which are weak nucleophiles and not prone to sequential monomer addition can be synthesized. The linking of the living PDMS homopolymer with the appropriate chlorosilane compound followed by the reaction with the living P2VP chains enabled the synthesis of PDMS-*b*-P2VP copolymers with targeted molecular weight values and well-defined characteristics. This platform methodology constitutes a significant synthetic advance that can be further applied to segments with similar nucleophilicity-related issues. We demonstrate an additional route to synthesize the PDMS-*b*-P2VP copolymers that are desirable for diverse applications not only due to the high immiscibility they present but also because of the ability of the pyridine moiety to be chemically modified leading to novel functional materials.

The molecular and thermal characteristics were determined using size exclusion chromatography as well as proton nuclear magnetic resonance spectroscopy and differential scanning calorimetry, respectively. Table 1 summarizes the molecular as well as the thermal characteristics of the copolymers (the samples are abbreviated as DVP) as directly calculated through the above mentioned techniques.

Table 1. Molecular and thermal characteristics of PDMS-*b*-P2VP copolymers including number average molecular weight ($\bar{M}_n$), dispersity indices (Đ), mass fraction and volume fraction of PDMS (f_{PDMS} and ϕ_{PDMS} respectively) as well as the glass transition temperatures of the constituents.

Sample	$\bar{M}_n$ PDMS (a) (g/mol) SEC	$\bar{M}_n$ P2VP (a) (g/mol) SEC	$\bar{M}_n$ total (a) (g/mol) SEC	$Đ^{total}$ (a) SEC	f_{PDMS} (b) ^1H-NMR	ϕ_{PDMS} (b)	T_g^{PDMS} (c) (°C)	T_g^{P2VP} (c) (°C)
DVP-1	5,300	4,500	9,800	1.06	0.55	0.54	−125.75	84.55
DVP-2	15,500	7,000	22,500	1.05	0.68	0.67	−123.97	87.07
DVP-3	6,000	30,000	36,000	1.04	0.16	0.15	−121.98	102.41

(a) SEC in THF at 35 °C. (b) ^{1}H NMR measurements in $CDCl_3$ at 25 °C. The mass fraction ratio was calculated as follows:

$$f_{PDMS} = \frac{integration\ value_{0.1-0.5}}{contributing\ protons\ (or\ 6)} x\ monomeric\ unit\ molecular\ weight\ (or\ 74),$$

$$f_{P2VP} = \frac{integration\ value_{8.20}}{contributing\ protons\ (or\ 1)} x\ monomeric\ unit\ molecular\ weight\ (or\ 105).$$

Consequently the volume fraction is estimated through the following equations:

$\varphi_{P2VP} = \frac{f_{P2VP}\rho_{PDMS}}{f_{P2VP}\rho_{PDMS}+(1-f_{P2VP})\rho_{P2VP}}$, $\varphi_{PDMS} = \frac{f_{PDMS}\rho_{P2VP}}{f_{PDMS}\rho_{P2VP}+(1-f_{PDMS})\rho_{PDMS}}$, where ϱ_{P2VP}=0.975 g/cm^3 and ϱ_{PDMS}=0.970 g/cm^3.

(c) DSC experiments.

As showcased in the relative chromatographs (Figure 2a), monomodal distributions were received for the final copolymers in the three different cases indicating the absence of any undesired by-product prior to the self-assembly studies. The ^{1}H NMR spectra further revealed the blocks' composition through the integration of the characteristic proton signals of each monomeric unit. Specifically at δ: 0.1-0.5 ppm, the chemical shifts are assigned to the six protons of the siloxane side methyl groups (C-H$_3$) while the peak area at δ: 8.2 ppm (Ar-H) corresponds to the proton of the aromatic ring of the pyridine moiety as indicated in Figure 2b. The targeted integrations in all spectra through which the mass and therefore the volume fraction ratios can be calculated, are presented as well. The thermal characterization of the copolymers through DSC indicated two different glass transition temperatures at values similar to those of the relative homopolymers. The significant difference between the two T_gs, which is approximately 200 ^{o}C (lower than −121 ^{o}C and 100 ^{o}C for the PDMS and P2VP respectively), suggest the quite dissimilar properties of the components and therefore the strong repulsion between them. Any additional transitions are allocated to the melting and cold crystallization of the PDMS crystals. To calculate the degree of crystallinity of the PDMS crystals during melting in the DVP-1 and DVP-2, the enthalpy of fully crystallized PDMS was considered equal to 37.4 J/g based on the literature [26,27], leading to 19% and 25% of crystalline chains respectively. The thermographs with the different thermal transitions are presented in Figure 2c.

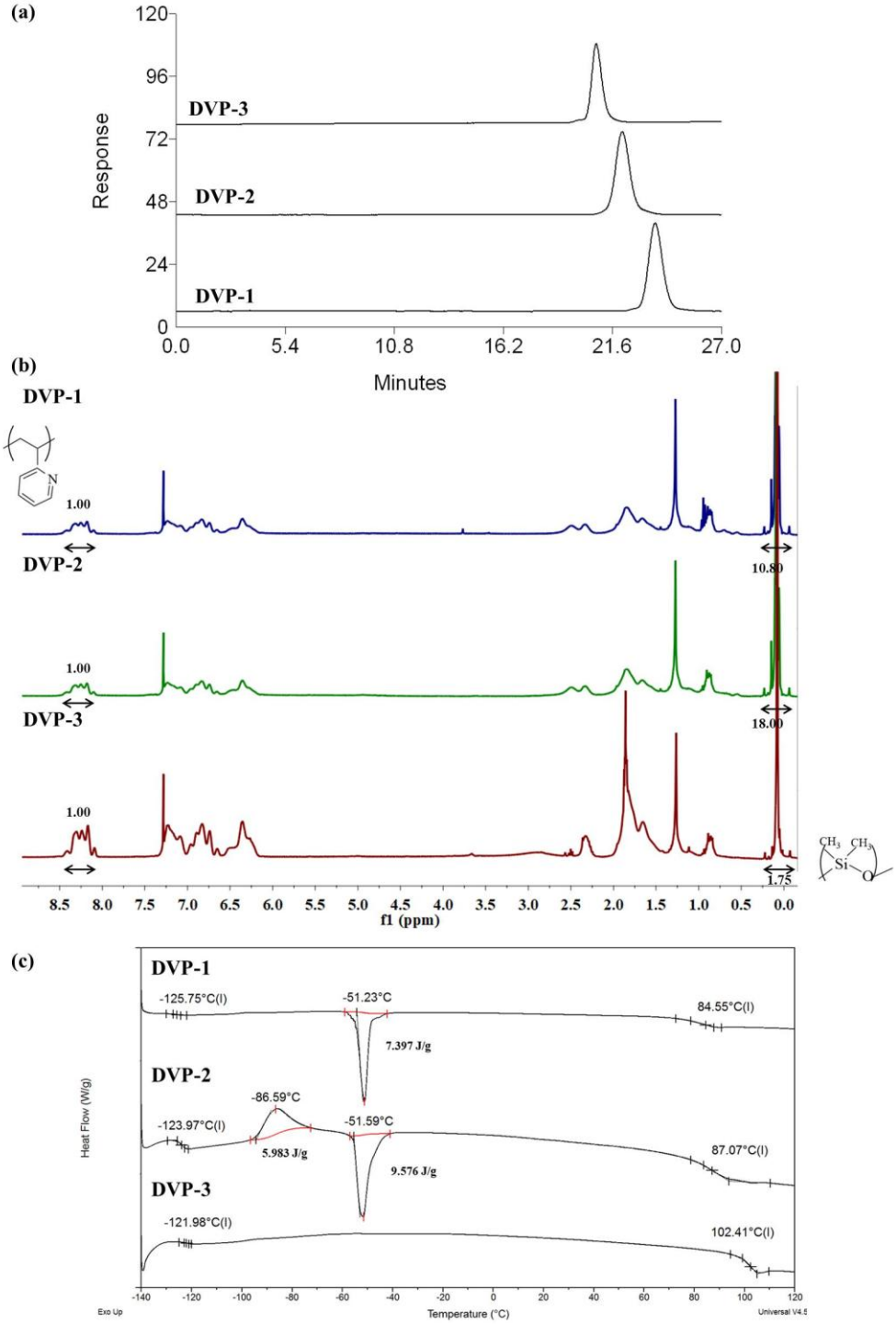

Figure 2. (a) Chromatographs, (b) ^{1}H NMR spectra and (c) thermographs of all synthesized copolymers as taken from the corresponding characterization techniques.

To establish a relationship between molecular characteristics and self-assembly behavior, TEM and SAXS experiments were conducted. The samples were cast in chloroform which is more selective for the P2VP block if one takes into consideration the solubility parameters (chloroform: 18.7 MPa$^{1/2}$, PDMS: 15.5 MPa$^{1/2}$ and P2VP: 20.6 MPa$^{1/2}$) [7,13,28] and left to evaporate at ambient conditions. The contrast obtained by silicon atoms in PDMS and carbon atoms in P2VP allowed for TEM observations without selective staining with iodine. All as-cast samples were studied without being submitted to

thermal annealing since copolymers showcase the highest repulsion at lower temperatures. The results are summarized in Figure 3.

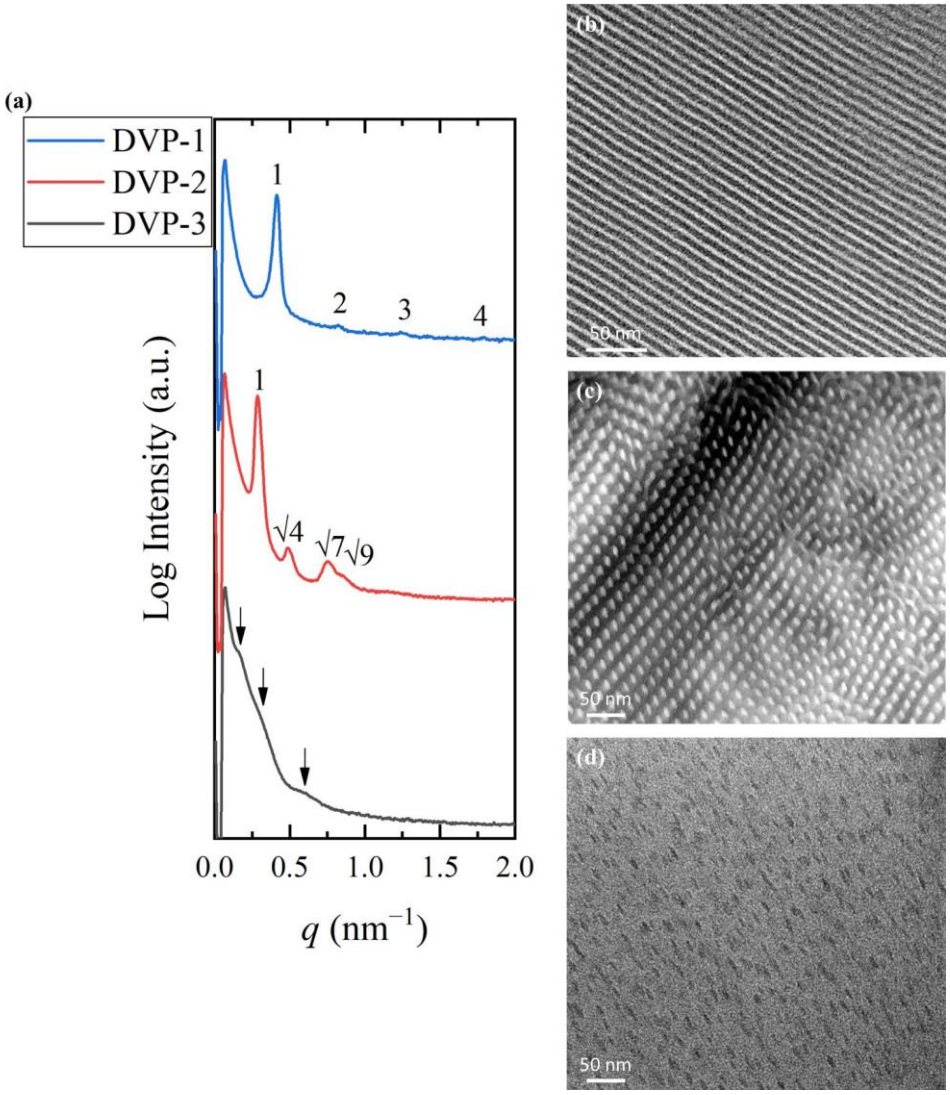

Figure 3. (a) 1D SAXS profiles of DVP-1 (blue), DVP-2 (red) and DVP-3 (black). TEM micrographs of (b) DVP-1, (c) DVP-2 and (d) DVP-3 demonstrating alternating lamellae, hexagonal packed cylinders and a spherical phase respectively. The dark domains correspond to the PDMS and white/grey to the P2VP in all cases.

DVP-1 formed alternating lamellae sheets as indicated by the 1D SAXS profile and the relative TEM micrograph after solution casting in chloroform (Figure 3a blue line and 3b respectively). The black periodic regions correspond to the PDMS domains while the white stripes to the P2VP. The characteristic reflections at the relative q values of 1:2:3 further corroborated the real-space imaging results. The domain periodicity was calculated using the sharp primary reflection through Bragg's law equal to 15.2 nm. The small dimensions obtained demonstrate the ability of the specific sequence to self-assembly despite the low degree of polymerization and therefore the strong immiscibility between the divergent components is verified.

The self-assembly studies on the DVP-2 suggested the formation of hexagonal packed cylinders of the minority component or P2VP (white areas) inside the black PDMS matrix as indicated in the relative TEM micrograph (Figure 3b). The reciprocal space results further confirmed the cylindrical morphology if one takes into consideration the characteristic reflections at the relative q values of 1: $\sqrt{4}$: $\sqrt{7}$: $\sqrt{9}$. The domain

spacing was calculated through the principal reflection equal to 21.9 nm (Figure 3a red line).

DVP-3 showcases the highest asymmetry between the molecular characteristics of the involved segments which is also depicted in the morphological characterization results. Specifically, the copolymer adopted the spherical morphology as it can be observed in the respective micrograph (Figure 3c) but no long range order was accomplished as indicated by the absence of sharp reflections in the corresponding 1D SAXS plot (Figure 3a black line). Besides the lack of ordered domains, no solid results concerning the formed structure can be extracted due to the broad peaks which do not allow for the appropriate peak assignment. The broad nanodomain boundaries are indicated from the weak intensity of peaks and reveal that the copolymer is not strongly segregated. The domain spacing was calculated equal to 39 nm using the first permitted reflection.

Taking into consideration the experimental results one can assume that the specific copolymer sequence adopts hexagonal and lamellar phases for common volume fraction ratios while the highest asymmetry between the compositions of the components induced the formation of spherical morphology without long range order.

DVP-3, as already mentioned in a previous section, was submitted to a quaternization reaction due to its higher content in P2VP (ϕ_{P2VP}=0.85) comparing to the remaining copolymers, leading to PDMS-*b*-[P2VP-*r*-poly(1-ethyl-2-vinylpyridinium bromide)] or DVP-3q. The sample was further characterized at molecular level through infrared spectroscopy to map any alternation on the absorption bands prior and after the quaternization. In the spectrum of the pristine copolymer, the absorption signals corresponding to the characteristic P2VP and PDMS groups are evident. In particular, the signals at 3000-3100 cm^{-1} indicate the presence of aromatic C-H stretching and at 1400 and 1450 cm^{-1} the C=C stretching. The signals at 570 and 750 cm^{-1} correspond to the deformation of the aromatic ring. Also, at 1070-1340 cm^{-1} C-N stretching vibrations can be identified. PDMS exhibit IR peaks at approximately 700-796 cm^{-1} due to the -CH_3 rocking and Si-C stretching, at 1020-1074 cm^{-1} because of the Si-O-Si stretching and finally at 1260–1259 cm^{-1} as well as at 2950-2960 cm^{-1} due to the -CH_3 deformation and asymmetric -CH_3 stretching in Si-CH_3 group respectively. For the DVP-3q additional absorptions in the range between 1070 and 1340 cm^{-1} are emerging which are attributed to C-C stretching vibrations in the ethyl group of bromoethane. The comparative spectra are presented in Figure 4a.

Based on literature [15] the reaction of P2VP-containing copolymers with bromoethane yields a 20% quaternization extent. The close proximity of the nitrogen atom to the backbone and therefore enlarged steric hindrance does not allow higher yields, therefore unmodified and quaternized monomeric units coexist in the P2VP segment. The results obtained from ^{1}H NMR studies corroborated the ones mentioned in literature [15]. Specifically, the DVP-3q was dissolved in DMSO-d_6 since quaternized pyridine blocks demonstrate better solubility in a more polar solvent. In the relative spectrum (Figure 4b) the emergence of an additional peak at approximately 8.95 pm is allocated to the chemical shift of the proton corresponding to the quaternary ammonium group. The quantitative analysis of the quaternized and non-quaternized peaks indeed revealed that the yield of the reaction was equal to 20%.

DSC experiments on the modified copolymer indicated a slight increase on the T_g of the P2VP segments. This phenomenon can be explained by the introduction of bromoethane compound into certain polymer chains, which possibly led to an enhancement on intermolecular interactions. Also, the alternation on the thermal transition is not significant due to the low extent of quaternization. The thermograph of the quaternized copolymer is presented in Figure 4c.

The wetting properties of both DVP-3 and DVP-3q in thin films state were evaluated using water contact angle measurements. The introduction of bromoethane in the pyridine moiety increased the overall polarity of the sample even though the quaternization

yield did not exceed 20%. Specifically, the contact angle of the neat copolymer was calculated approximately 95° (±2°) while the modified sample exhibited decreased water contact angle ca. 83° (±2°). The different surface properties of the DVP-3q are allocated to the secondary interactions (such as hydrogen bonds and dipole-dipole interactions) between the O-H bonds of water and the quaternized groups in some of the P2VP monomeric units. The results are presented in Figure 4d.

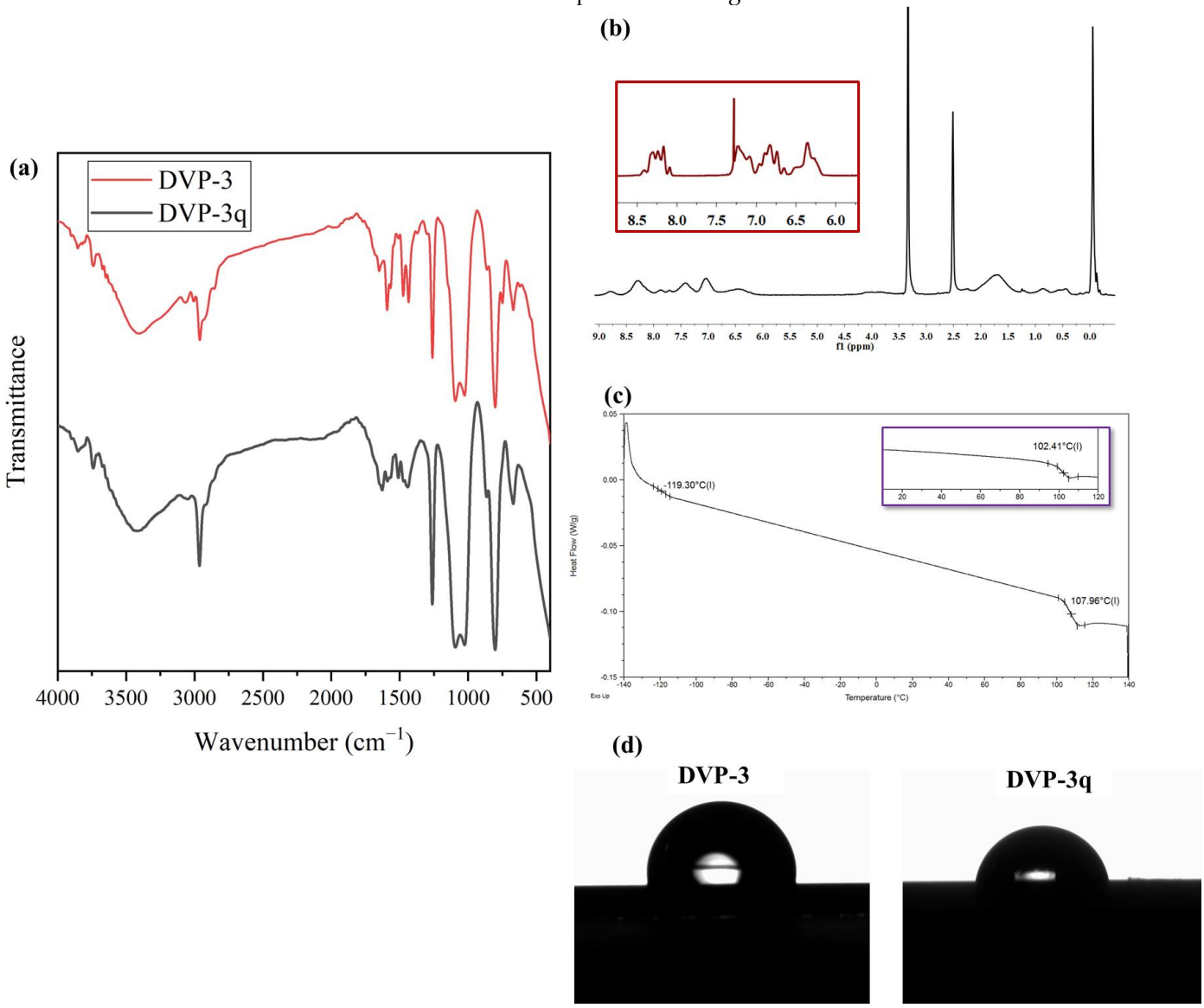

Figure 4. (a) Comparative FT-IR spectra of DVP-3 (red) and DVP-3q (black). (b) ^{1}H NMR spectrum of DVP-3q in DMSO-d$_6$. The inlet in red corresponds to the ^{1}H NMR spectrum (in chloroform) of the neat copolymer and is presented for comparison reasons (c) DSC thermograph of DVP-3q. The inlet in purple corresponds to the thermograph of the neat copolymer to indicate the temperature differentiation in the T$_g$s before and after quaternization (d) Water contact angle measurements of DVP-3 [95° (±2°)] and DVP-3q [83° (±2°)].

4. Conclusions

We propose a platform methodology to synthesize copolymers with segments presenting nucleophilicity-related issues through anionic polymerization. In particular, the living anionically synthesized homopolymer chains (i.e. PDMSLi$^+$ and P2VPLi$^+$) are covalently joined *via* chlorosilane chemistry leading to narrow dispersed PDMS-*b*-P2VP copolymers. Each step, during the different reactions, requires meticulous manipulations in terms of purification and vacuum quality to avoid the deactivation of reagents and the

appearance of side reactions. The samples were characterized molecularly and thermally to determine the molecular weight values, dispersity indices, composition and thermal transitions including glass transition temperatures as well as melting and crystallization temperature of PDMS crystals, where evident. The solid state properties of the copolymers were studied through TEM and SAXS showcasing the self-assembly capacity of the specific system. The composition of the components allowed for the formation of lamellar- and cylindrical- shaped structures with approximately 15 nm and 21 nm spacings respectively. Also, the highest asymmetry with respect to the segment's content gave rise to a spherical morphology with d value equal to 39 nm. The materials are potential candidates for nanotechnology applications due to the enhanced immiscibility of the constituents. The presence of nitrogen atom in the P2VP moiety may possible lead to the preparation of functional materials simply by conducting post polymerization chemical modification reactions.

Author Contributions: Conceptualization, A.A.; methodology, G.-M.M., I.M., D.M., C.N. and A.A.; validation, D.A.I. and A.A.; formal analysis, G.-M.M., I.M. and A.A.; investigation, G.-M.M., I.M., D.M., M.R., L.V. and A.A.; resources, D.A.I. and A.A.; data curation, G.-M.M., I.M., D.M., G.P., C.N., M.R., L.V., G.G.A., D.A.I. and A.A.; writing—original draft preparation, G.-M.M., I.M. and A.A.; writing—review and editing, G.-M.M., I.M., D.A.I. and A.A.; supervision, A.A.; funding acquisition, D.A.I. and A.A. All authors have read and agreed to the published version of the manuscript.

Funding: The chemical synthesis part of the work was financially supported by the Ministry of Science and Higher Education of the Russian Federation within State Contract 075-15-2022-1105. The structural characterization part of the work was supported by the Ministry of Science and Higher Education of the Russian Federation (Agreement 075-10-2021-093, Project BMA-RND-2009). The research work was partially supported by the Hellenic Foundation for Research and Innovation (HFRI) under the 3rd Call for HFRI PhD Fellowships (Fellowship Number: 6854).

Institutional Review Board Statement: Not applicable.

Data Availability Statement: The data presented in this study are available upon request from the corresponding author.

Acknowledgments: I.M., G.-M.M., D.M., G.P., C.N. and A.A. would like to acknowledge the Network of Research Supporting Laboratories at the University of Ioannina for using the Electron Microscopy Facility and the Nuclear Magnetic Resonance Spectroscopy Center. I.M., M.R., and D.A.I. would like to acknowledge the Dual Belgian Beamline (DUBBLE) of the European Synchrotron Radiation Facility (E.S.R.F.).

Conflicts of Interest: The authors declare no conflict of interest.

References

1. Angelopoulou, P. P.; Moutsios, I.; Manesi, G. M.; Ivanov, D. A.; Sakellariou, G.; Avgeropoulos, A. Designing High χ Copolymer Materials for Nanotechnology Applications: A Systematic Bulk vs. Thin Films Approach. *Prog. Polym. Sci.* **2022**, *135*, 101625. https://doi.org/10.1016/j.progpolymsci.2022.101625.
2. Lo, T. Y.; Krishnan, M. R.; Lu, K. Y.; Ho, R. M. Silicon-Containing Block Copolymers for Lithographic Applications. *Prog. Polym. Sci.* **2018**, *77*, 19–68. https://doi.org/10.1016/j.progpolymsci.2017.10.002.
3. Sinturel, C.; Bates, F. S.; Hillmyer, M. A. High χ-Low N Block Polymers: How Far Can We Go? *ACS Macro Lett.* **2015**, *4* (9), 1044–1050. https://doi.org/10.1021/acsmacrolett.5b00472.
4. Cummins, C.; Ghoshal, T.; Holmes, J. D.; Morris, M. A. Strategies for Inorganic Incorporation Using Neat Block Copolymer Thin Films for Etch Mask Function and Nanotechnological Application. *Adv. Mater.* **2016**, *28* (27), 5586–5618. https://doi.org/10.1002/adma.201503432.
5. Bellas, V.; Iatrou, H.; Hadjichristidis, N. Controlled Anionic Polymerization of Hexamethylcyclotrisiloxane. Model Linear and Miktoarm Star Co- and Terpolymers of Dimethylsiloxane with Styrene and Isoprene. *Macromolecules* **2000**, *33* (19), 6993–6997. https://doi.org/10.1021/ma000635i.
6. Chao, C. C.; Wang, T. C.; Ho, R. M.; Georgopanos, P.; Avgeropoulos, A.; Thomas, E. L. Robust Block Copolymer Mask for Nanopatterning Polymer Films. *ACS Nano* **2010**, *4* (4), 2088–2094. https://doi.org/10.1021/nn901370g.

7. Jeong, J. W.; Park, W. I.; Kim, M. J.; Ross, C. A.; Jung, Y. S. Highly Tunable Self-Assembled Nanostructures from a Poly(2-Vinylpyridine-b-Dimethylsiloxane) Block Copolymer. *Nano Lett.* **2011**, *11* (10), 4095–4101. https://doi.org/10.1021/nl2016224.
8. Kim, J. M.; Hur, Y. H.; Jeong, J. W.; Nam, T. W.; Lee, J. H.; Jeon, K.; Kim, Y.; Jung, Y. S. Block Copolymer with an Extremely High Block-to-Block Interaction for a Significant Reduction of Line-Edge Fluctuations in Self-Assembled Patterns. *Chem. Mater.* **2016**, *28* (16), 5680–5688. https://doi.org/10.1021/acs.chemmater.6b01731.
9. Pitet, L. M.; Wuister, S. F.; Peeters, E.; Kramer, E. J.; Hawker, C. J.; Meijer, E. W. Well-Organized Dense Arrays of Nanodomains in Thin Films of Poly(Dimethylsiloxane)-b-Poly(Lactide) Diblock Copolymers. *Macromolecules* **2013**, *46* (20), 8289–8295. https://doi.org/10.1021/ma401719p.
10. Luo, Y.; Montarnal, D.; Kim, S.; Shi, W.; Barteau, K. P.; Pester, C. W.; Hustad, P. D.; Christianson, M. D.; Fredrickson, G. H.; Kramer, E. J.; Hawker, C. J. Poly(Dimethylsiloxane-b-Methyl Methacrylate): A Promising Candidate for Sub-10 Nm Patterning. *Macromolecules* **2015**, *48* (11), 3422–3430. https://doi.org/10.1021/acs.macromol.5b00518.
11. Azuma, K.; Sun, J.; Choo, Y.; Rokhlenko, Y.; Dwyer, J. H.; Schweitzer, B.; Hayakawa, T.; Osuji, C. O.; Gopalan, P. Self-Assembly of an Ultrahigh-χ Block Copolymer with Versatile Etch Selectivity. *Macromolecules* **2018**, *51* (16), 6460–6467. https://doi.org/10.1021/acs.macromol.8b01409.
12. Luo, Y.; Kim, B.; Montarnal, D.; Mester, Z.; Pester, C. W.; McGrath, A. J.; Hill, G.; Kramer, E. J.; Fredrickson, G. H.; Hawker, C. J. Improved Self-Assembly of Poly(Dimethylsiloxane-b-Ethylene Oxide) Using a Hydrogen-Bonding Additive. *J. Polym. Sci. Part A Polym. Chem.* **2016**, *54* (14), 2200–2208. https://doi.org/10.1002/pola.28093.
13. Kennemur, J. G. Poly(Vinylpyridine) Segments in Block Copolymers: Synthesis, Self-Assembly, and Versatility. *Macromolecules* **2019**, *52* (4), 1354–1370. https://doi.org/10.1021/acs.macromol.8b01661.
14. Mavronasou, K.; Zamboulis, A.; Klonos, P.; Kyritsis, A.; Bikiaris, D. N.; Papadakis, R.; Deligkiozi, I. Poly(Vinyl Pyridine) and Its Quaternized Derivatives: Understanding Their Solvation and Solid State Properties. *Polymers* **2022**, *14* (4). https://doi.org/10.3390/polym14040804.
15. Carrasco, P. M.; Ruiz De Luzuriaga, A.; Constantinou, M.; Georgopanos, P.; Rangou, S.; Avgeropoulos, A.; Zafeiropoulos, N. E.; Grande, H. J.; Cabañero, G.; Mecerreyes, D.; Garcia, I. Influence of Anion Exchange in Self-Assembling of Polymeric Ionic Liquid Block Copolymers. *Macromolecules* **2011**, *44* (12), 4936–4941. https://doi.org/10.1021/ma200213s.
16. Lee, J.; Hogen-Esch, T. E. Synthesis and Characterization of Narrow Molecular Weight Distribution AB and ABA Poly(Vinylpyridine)-Poly(Dimethylsiloxane) Block Copolymers via Anionic Polymerization. *Macromolecules* **2001**, *34* (9), 2805–2811. https://doi.org/10.1021/ma001439e.
17. Fragouli, P. G.; Iatrou, H.; Hadjichristidis, N. Synthesis and Characterization of Linear Tetrablock Quarterpolymers of Styrene, Isoprene, Dimethylsiloxane, and 2-Vinylpyridine. *J. Polym. Sci. Part A Polym. Chem.* **2004**, *42* (3), 514–519. https://doi.org/10.1002/pola.10856.
18. Hur, Y. H.; Song, S. W.; Kim, J. M.; Park, W. I.; Kim, K. H.; Kim, Y. J.; Jung, Y. S. Thermodynamic and Kinetic Tuning of Block Copolymer Based on Random Copolymerization for High-Quality Sub-6 Nm Pattern Formation. *Adv. Funct. Mater.* **2018**, *28* (28), 1–9. https://doi.org/10.1002/adfm.201800765.
19. Hur, Y. H.; Song, S. W.; Kim, J. M.; Park, W. I.; Kim, K. H.; Kim, Y. J.; Jung, Y. S. Thermodynamic and Kinetic Tuning of Block Copolymer Based on Random Copolymerization for High-Quality Sub-6 Nm Pattern Formation. *Adv. Funct. Mater.* **2018**, *28* (28), 1–9. https://doi.org/10.1002/adfm.201800765.
20. Cho, H.; Kim, S.; Park, S. Fabrication of Gold Nanoparticles and Silicon Oxide Corpuscles from Block Copolymers. *J. Mater. Chem.* **2010**, *20* (6), 1156–1160. https://doi.org/10.1039/b922334g.
21. Shi, L. Y.; Lei, W. W.; Liao, F.; Chen, J.; Wu, M.; Zhang, Y. Y.; Hu, C. X.; Xing, L.; Zhang, Y. L.; Ran, R. H-Bonding Tuned Phase Transitions of a Strong Microphase-Separated Polydimethylsiloxane-b-Poly(2-Vinylpyridine) Block Copolymer. *Polymer* **2018**, *153*, 277–286. https://doi.org/10.1016/j.polymer.2018.02.003.
22. Hadjichristidis, N.; Iatrou, H.; Pispas, S.; Pitsikalis, M. Anionic Polymerization: High Vacuum Techniques. *J. Polym. Sci. Part A Polym. Chem.* **2000**, *38* (18), 3211–3234. https://doi.org/10.1002/1099-0518(20000915)38:18<3211::AID-POLA10>3.0.CO;2-L.
23. Angelopoulou, P. P.; Kearney, L. T.; Keum, J. K.; Collins, L.; Kumar, R.; Sakellariou, G.; Advincula, R. C.; Mays, J. W.; Hong, K. High-χ Diblock Copolymers Containing Poly(Vinylpyridine-N-Oxide) Segments. *J. Mater. Chem. A* **2023**, *11* (18), 9846–9858. https://doi.org/10.1039/d3ta01386c.
24. Uhrig, D.; Mays, J. W. Experimental Techniques in High-Vacuum Anionic Polymerization. *J. Polym. Sci. Part A Polym. Chem.* **2005**, *43* (24), 6179–6222. https://doi.org/10.1002/pola.21016.
25. Liontos, G.; Manesi, G. M.; Moutsios, I.; Moschovas, D.; Piryazev, A. A.; Bersenev, E. A.; Ivanov, D. A.; Avgeropoulos, A. Synthesis, Molecular Characterization, and Phase Behavior of Miktoarm Star Copolymers of the ABnand AnB (n = 2 or 3) Sequences, Where A Is Polystyrene and B Is Poly(Dimethylsiloxane). *Macromolecules* **2022**, *55* (1), 88–99. https://doi.org/10.1021/acs.macromol.1c01863.
26. Klonos, P. A. Crystallization, Glass Transition, and Molecular Dynamics in PDMS of Low Molecular Weights: A Calorimetric and Dielectric Study. *Polymer* **2018**, *159*, 169–180. https://doi.org/10.1016/j.polymer.2018.11.028.
27. Aranguren, M. I. Crystallization of Polydimethylsiloxane: Effect of Silica Filler and Curing. *Polymer (Guildf).* **1998**, *39* (20), 4897–4903. https://doi.org/10.1016/S0032-3861(97)10252-X.
28. Lee, J. N.; Park, C.; Whitesides, G. M. Solvent Compatibility of Poly(Dimethylsiloxane)-Based Microfluidic Devices. *Anal. Chem.* **2003**, *75* (23), 6544–6554. https://doi.org/10.1021/ac0346712.

476